# Measurement and Modelling of Impurity Transport in Radiating Boundary Discharges in ASDEX Upgrade

R. Dux, A. Kallenbach, K. Behringer, R. Neu, S. de Peña-Hempel, M. Sokoll, and the ASDEX Upgrade-,NI- and ICRH-teams

MPI für Plasmaphysik, EURATOM Association, Garching & Berlin, Germany

## Introduction

Radiative cooling of the plasma boundary by controlled injection of medium Z impurities has been demonstrated to yield substantial reductions of the power flow onto the target plates as required for future reactors. Important key numbers for such scenarios are fuel dilution and central radiation loss caused by increased central density of the added impurity depending on the radial transport parameters of the impurity in the bulk plasma. Radiating boundary CDH-mode discharges in the ASDEX Upgrade tokamak with high-power neutral beam injection and neon as radiating species [1] were analyzed and the impurity transport in the plasma bulk was investigated.

## CDH-mode types of discharges with different bulk transport

A comparison of two CDH-mode discharges with neon is shown in fig. 1. Both discharges have plasma current $I_p$=1MA, toroidal field $B_T$=2.5T and safety factor $q_{95}$=4. Constant NBI-heating with $P_{NI}$=7.5MW is used and #8115 has additional 400kW central ICRH-heating. Neon is puffed into the main chamber and the neon puff rate $\Gamma_{Ne}$ is feedback controlled to reach a constant power fraction $P_{rad}/P_{heat}$ ≈0.9. With the increase of $P_{rad}$ the ELM-type changes from type-I to type-III and the plasma detaches from the target plates as indicated by the CIII signal measured directly above the outer target plate (CDH-mode).

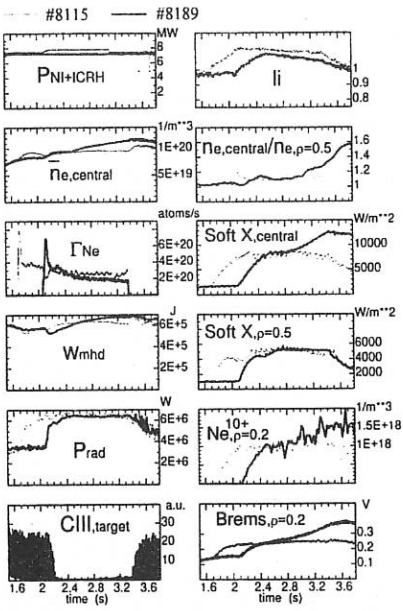


*Figure 1: Comparison of two CDH-discharges with different central transport behaviour.*

After the onset of the CDH-mode both discharges show similar behaviour for the first 0.4s. For the rest of the CDH-phase, however, the bulk transport for both discharges is very different. The electron density profile, represented by line-averaged values of a central line-of-sight and the density ratio $n_{e,central}/n_{e,rho=0.5}$, remains constant for #8115 while it peaks for #8189. The soft x-ray time traces of a central chord and a chord with $\rho_{pol,tan}$=0.5, stay nearly constant for #8115 and show a strong peaking for #8189. As will be shown later, this strong peaking of the soft x-ray profile for #8189 can only be explained by a central accumulation of neon. Some indication to this is also given by the density of the fully

ionized neon at $\rho_{pol}$=0.2 measured by charge exchange recombination spectroscopy and by visible bremsstrahlung measurement on a chord with $\rho_{pol,tan}$=0.2. The internal inductivity $l_i$ is a measure of the current profile peaking. For #8189 lower $l_i$ values, i.e. flatter current profiles, are observed due to higher resistivity in the plasma center: $\eta \propto Z_{eff} T_e^{-3/2}$. The stored energy $W_{mhd}$ reaches higher values in the case of peaked electron and impurity density profiles(#8189).

The development of the peaking in #8189 is accompanied by a suppression of sawteeth and the growth of an m=1-mode while #8115 shows strong sawteeth during the whole discharge. In a number of radiating boundary discharges (CDH-mode and H-mode) with parameters nearly identical to the ones presented here sawteeth are always found to suppress central peaking of electron density and neon while the lack of sawteeth always leads to peaked profiles. When reaching high levels of radiated power fraction the plasma is very close to the limit of sawtooth instability. We observed discharges with and without sawteeth in type-I ELM'y H-modes as well as in CDH-modes. For L-mode the database is not very large, but here sawteeth were always present. Triggering of sawteeth by central ICRH-heating could not clearly be seen for the heating powers reached so far ($\approx 500kW$).

### Modelling of Impurity Transport in the Case of no Sawteeth

The neon transport and radiation has been modelled with the radial impurity transport code STRAHL [2] using atomic data from the ADAS [3] database. The code uses measured profiles of electron density and temperature in the main plasma, the scrape-off layer is treated in a simplified manner applying decay lengths which are fitted to measured data. The radial transport equations are solved by an ansatz of anomalous and/or neoclassical diffusivities and radial drift velocities. The neon source function is evaluated from the measured valve fluxes using an empirical description of recycling and pumping with a simple chamber model [4].

In fig. 2 various profiles are given for three time points of the discharge #8189 and are compared with measured values. The first time point represents the case with flat impurity profile and sustained sawtooth action, the second with peaked impurity profile at the end of the CDH-mode shortly before the neon puff stops and the third 0.5 s after neon puffing. The total neon density and the according $\Delta Z_{eff}$ is shown in fig. 2a and 2b. Fig. 2d gives the measured electron densities for these times. Note that the peaking of neon coincides with a peaking of the electron density.

Fig. 2c and 2e show a comparison of measured and calculated radiation fluxes for two soft x-ray pinhole cameras, which cover the total poloidal plasma cross section, plotted over the minimal poloidal flux label of the according line-of-sight (negative flux labels for chords below the plasma center). One camera is equipped with an $8\mu m$ thick beryllium filter, cutting out all radiation below ≈1keV. It is sensitive to line radiation of hydrogen-like and partly helium-like neon ions, but from all other ionization stages of neon and from other lighter impurities only bremsstrahlung and recombination radiation contribute. The other camera has a $100\mu m$ thick beryllium filter, which makes the camera insensitive for all line radiation of the light impurities due to an energy limit of ≈2.5keV. Thus the $100\mu m$-camera observes always peaked profiles, while the $8\mu m$-camera measures hollow or peaked profiles because there is always a second maximum of the emissivity around $\rho_{pol}$=0.85 due to line radiation of H- and He-like neon. The signals of both cameras are dominated by the neon radiation and the neon on/off ratios are about 5:1 to 10:1. The background radiation due to intrinsic impurities was treated by just considering carbon

and adjusting the carbon level to such a level, that the pre-puff radiation profiles could be fitted. Then the transport parameters for Ne and C were adjusted to get the best agreement of the modelled and measured soft x-ray radiation fluxes.

In fig. 2g the modelled densities of fully ionized neon are shown together with the measured values from charge exchange recombination spectroscopy (CXRS). The fit to the soft x-ray data gives also good agreement with the CXRS-data. Unfortunately the innermost point at $\rho_{pol}$=0.11 has a high uncertainty due to low signal.

As one can see from the time traces in fig. 1, the impurity peaking coincides with a peaking of the electron density. Thus we tested, whether the impurity profiles can be explained by neoclassical pinch terms being proportional to the slope of the proton profile ($v_{drift,neo} \propto dn_p/dr$), which in turn is self-consistently modelled from the given electron density and the impurity density (drifts due to friction between impurities were neglected). However, since the profile shape is determined by the ratio of drift velocity and diffusivity a serious test can only be performed when the anomalous diffusion coefficient $D_{an}$ is known. In former investigations [5] we found hollow profiles for the diffusion coefficient with central values of 2-3 times the neoclassical value (thick grey line in fig. 2f), however, these values are sawtooth-averaged. Now we assumed that in the sawtooth-free period of the discharge the diffusion reduces to neoclassical values in the center (solid line in fig. 2f). With this low central diffusion and by increasing the neoclassical drift velocities by a factor of 1.5 (fig. 2h) the peaking of impurity and soft x-ray emission could be described. The gradients of $T_e$ and $n_e$ are rather uncertain in the steep gradient zone $\rho_{pol} > 0.9$ and only anomalous transport was used in this region.

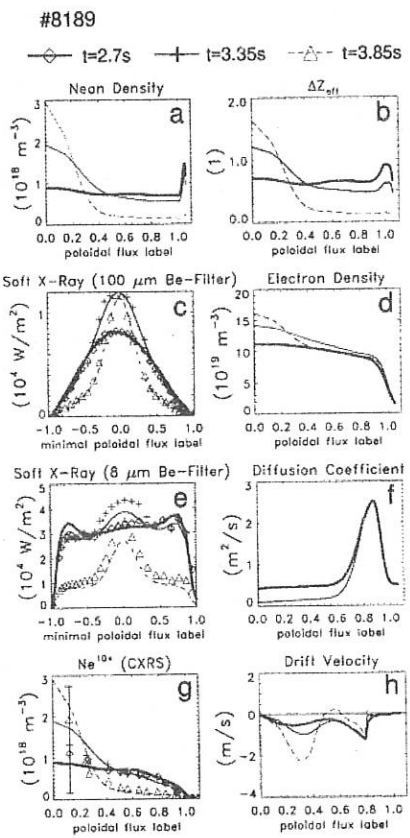


*Figure 2: Neon density and soft-x radiation profiles for three time points of discharge #8189 modelled with impurity transport code STRAHL in comparison with measured profiles.*

Due to the uncertainties in the profiles of density, temperature, safety factor and anomalous diffusion this analysis of impurity peaking in terms of neoclassical theory is certainly not a real quantitative check but the qualitative features of the strong impurity peaking are described well.

### Central Impurity Transport with Sawteeth

For a first investigation of sawteeth induced impurity transport in discharge #8115 an unfolding of the additional soft x-ray radiation fluxes after the neon puff (measured with $100\mu m$ Be-filter) was performed assuming constant emissivity on flux surfaces. Fig. 3b shows the large modulation of the central soft x-ray emission in comparison to the variation of the central electron temperature in fig. 3c and the electron density in fig. 3a. From the soft x-ray emissivities the total neon densities in the center and at $\rho_{pol}$=0.5 (fig. 3d) were calculated taking into account the central variation of $T_e$ while at $\rho_{pol} = 0.5$ constant $T_e$ was used. It is clearly seen that in the CDH-phase every sawtooth leads to a completely flattened or even slightly hollow profile, which develops into a peaked profile until the onset of the next sawtooth. Just after the neon puff starts the neon profile is of course hollow and the sawteeth cause central filling of the neon profile. These observations are consistent with the picture that sawteeth produce a mixing of the impurity inventories inside and outside the q=1-radius [6]. From the time constant for profile recovery after a sawtooth crash and the sawtooth frequency the peaking for zero frequency can be calculated being only ≈10% higher than the observed mean peaking. Thus, even between sawtooth crashes the central transport of #8115 has a lower inward drift parameter compared with #8189 because $n_e$ is only slighlty peaked.

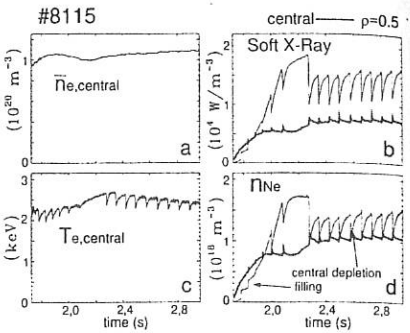


*Figure 3: Sawtooth modulations of neon densities evaluated from the variation of soft x-ray emissivity, electron density and temperature.*

### Conclusions

For CDH-mode discharges in ASDEX Upgrade neon density profiles have been determined from soft x-ray measurements using the impurity transport/radiation code STRAHL. For constant radiated power the central neon density varies strongly for discharges with and without sawteeth. All discharges in ASDEX-Upgrade with high radiation level are close to the stability limit of sawteeth. For discharges without sawteeth there is a strong neon peaking which can be explained qualitatively by neoclassical drifts due to peaked proton profiles. For discharges with sawteeth the neon peaking is reduced. The neon inventories inside and outside the q=1-radius are effectively mixed during a sawtooth crash. Only CDH-modes with sawteeth and flat electron profiles give useful values of $\Delta P_{rad}/\Delta Z_{eff}$ [7] and further experiments to preserve sawteeth by central heating will be performed.

### References

[1] J. Neuhauser et al., PPCF. **37** Suppl. 11A, A37 (1995).
[2] K. Behringer, JET-R(87)08, JET Joint Undertaking , Culham (1987).
[3] H. P. Summers, JET-IR 06, Jet Joint Undertaking, Culham (1994).
[4] R. Dux et al., to appear in PPCF. [5] A. Kallenbach et al., Nucl. Fus., **35** 1231 (1995).
[6] A. Ödblum et al., Phys. Plasmas, **3** 956 (1996). [7] A. Kallenbach et al., this conference.